Experimental Investigation of Two Types Interconnected Hydro-Pneumatic Struts

DEZHAO LIN[1], FAN YANG[1], DI GONG[1], FENG ZHAO[1], XIANGYU LUO[2], RUIHONG LI[1], AND ZHIHONG LIN[1]

[1]College of Mechanical Engineering and Automation, Huaqiao University, Xiamen 361021, China
[2]College of Computer Science and Technology, Huaqiao University, Xiamen 361021, China

Corresponding author: Fan Yang (xmyf@hotmail.com)

ABSTRACT The dynamic properties of two types of interconnected hydro-pneumatic struts (HPSs), which are designed based on two different types of the HPSs with integrated gas chamber, have been investigated through the setup experiment on the designed prototypes and established numerical model on the basis of the AMEsim software in this research work. Detailed analysis of the dynamic properties has been posted on the experimental data, including the in-phase and out-of-phase tests. Special emphasis has been placed on the analysis of some unusual phenomenon shown in the experiment, such as the negative output force, output force distortion, and small stiffness, and so on, which are seldom reported by researchers in this area. Then, the effect of the structural parameters, which include the length/diameter of the interconnected pipes and the size of orifices, to the dynamic properties, especially to the unusual phenomenon shown in the experiment, will be discussed through the established AMEsim model, in which the validity of the AMEsim model has been verified through the experiment. The presented research work provides the fundamental investigation on two types of interconnected HPSs, which have great potential application in the area of a vehicle suspension system.

INDEX TERMS Interconnected hydro-pneumatic strut, suspension, dynamic properties.

I. INTRODUCTION

As the demand of maneuverability and comfort to commercial vehicles is of greater concern, vehicle's suspension, which can solve the conflict between ride comfort and vehicle handling which is present in conventional suspension systems, has been widely investigated. Besides, the large variations in operating loads and operating conditions in vehicles require suspensions with variable characteristics. A semi-active/active suspension, with controllable stiffness and/or damping, such as Magneto-Rheological dampers, can be adjusted according to vehicle states to achieve improved vehicle ride and handle performances simultaneously [1]. The performance of a semi-active/active suspension strongly rely on not only its semi-active/active devices, but the related control methodologies. A wide variety of different controller synthesis has been reported for semi-active/active suspension

controller designs such as Skyhook damping control [2], neural network control [3], [4], Fuzzy control [5], [6]. Here, it should be noted that the commercial applications of semi-active/ active suspension haves been limited because of its high cost.

The mechanically/hydraulically interconnected suspension is the other kinds of device to balance the ride and handling performance of vehicles [7], [8]. Comparing with the traditional mechanically interconnected suspension, for example the anti-roll bar, hydraulically interconnected suspension (HIS) could offer even greater design flexibility by introducing fluid couplings among different chambers in/between different suspension strut units [9], and has small structural changing and less unsprung mass [10]. Some studies have also shown that HIS can yield significantly higher roll mode stiffness and damping with soft vertical ride performance [11]. Therefore, HIS has been widely studied and applied on Heavy Duty Vehicles. The recent researches all showed that HIS, in some contents, can improve the designed

compromise between handling performance and ride comfort under the working condition that the full-car suspension is in bounce-, roll-, pitch-, dual-modes [12]–[18]. For example, Hou *et al.* investigate the stiffness characteristic of HIS and the results shows that HIS can bitterly improve vehicles' rolling resistance [12]. Zhang *et al.* utilized a 4-DOF half-car model, which integrated a typical anti-roll HIS system, to investigate the modal stiffness and damping characteristics [13]. Smith *et al.* applied the HIS to a 9-DOF vehicle model to assess the handling performance [14]. Ding *et al.* investigated the characteristics of pitch-resistant HIS systems for two-axle vehicles in the pitch plane [15], and proposed a new HIS to enhance the roll dynamics of the tri-axle straight trucks [16]. Yao *et al.* used the hydraulic circuit flow-pressure relationships to derive a mathematical model for a dual-mode interconnected suspension [17]. Lam *et al.* proposed a fuzzy control methodology applying to HIS on the full-car model, and experimental results show that HIS can effectively reduce the pitch motion and prevent rollover [18]. The above studies are all related to the HIS strut with external gas chambers (accumulators), which are usually arranged in the interconnected hydraulic pipes. Wu proposed a novel hydro-pneumatic strut (HPS), as shown in Fig. 1(b) for left (*L*) or right (*R*) strut, in which the HPS is integrated with one internal gas accumulator [19]. Recently, Zhang *et al.* used statistical linearization to analyze the nonlinearity of this type of HPS and investigated the effect of the structural parameters through mathematical model [20]. Jiao *et al.* investigated the effect of environmental temperature to the properties of this type of HPS through established numerical model [21]. Based on the analysis of single HPS shown in Fig 1(b), Wu investigated the dynamic properties of the interconnected hydro-pneumatic strut (IC HPS), as show in Fig. 1(a), in which the orifices between the main and annular chambers of struts have been cancelled comparing with those shown in Fig. 1(b), and the results show that this type of IC HPS can provide good anti-roll properties [19]. Cao *et al.* presented set of investigation focusing on the anti-roll and anti-pitch properties, handling performance and ride comfort on the IC HPS shown in Fig. 1(a) considering the fluid compressibility based on the simulation [9], [22]–[24]. Since then, although the research papers regarding the IC HPS continuous appearing, based on the researcher's investigation on available literatures, the research of the two types of IC HPS investigated in this study shown in Fig. 1, looks discontinued, and it is still lack of experimental verification on these kinds of HPS or IC HPS.

Considering the above, this paper will propose one IC HPS, as illustrated in Fig. 1(b), based on the fundamental strut design proposed by Wu [19], and investigate the dynamic properties of two types of IC HPS, as illustrated in Fig. 1, based on the experiment on the designed prototypes, and the numerical model on AMEsim software. The equations of motion, derived through the force balance, volume conservation and the polytrophic process of gas, will be summarized in Chapter 2. Chapter 3 will present the design parameters
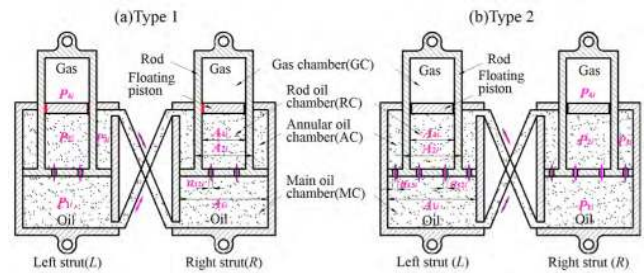

FIGURE 1. The structural diagram of two types interconnected hydra-pneumatic suspension strut.

of the prototypes, the established numerical model based on AMEsim software, and the set-up experimental platform. The dynamic properties obtained through set-up experiment will be presented, and then analyzed in Chapter 4. Based on the result presented in Chapter 4, Chapter 5 will focus on the analysis of effect of structural parameters to the dynamic properties of IC HPS. The result shows that the Type 2 IC HPS, as illustrated in Fig. 1(b), is able to provide good stiffness and damping properties with stable working properties through suitably designed structural parameters, which will be summarized in the last chapter. The presented work provides the fundamental investigation of the two types of IC HPS based on the experimental data, and provide advising for the practical application of these kind of IC HPS.

II. MODELLING OF TWO TYPES OF INTERCONNECTED HYDRO-PNEUMATIC STRUTS

Fig. 1 illustrates the structural diagram of two types of interconnected hydro-pneumatic strut (IC HPS), which will be investigated in this paper. The first type of IC HPS (Type 1), as illustrated in Fig. 1(a), was proposed by Wu [19]. The fundamental strut design for Type 2 IC HPS, as shown in Fig. 1(b), was also proposed by Wu [19], and its interconnected working condition will be investigated in this study, as well.

A. MODELING OF TYPE 1 IC HPS

Two identical HPS (*L*, *R*) shown in the Fig. 1(a), originally proposed by Wu [19], assemble the Type 1 IC HPS, and its dynamic properties has been studies based on mathematical model [19]. The HPS is integrated with one internal gas accumulator and one group of orifices between the main oil chamber (MC) and the rod oil chamber (RC). The MC of strut *L* (or *R*) and annular oil chamber (AC) of strut *R* (or *L*) are connected through hydraulic pipes, as illustrated in Fig. 1(a). Therefore, the oil can be moved between MC and RC in one strut, and MC and AC among struts. The oil flow between MC and RC will change the volume of the inert gas (nitrogen gas) chamber (GC), and then provide the stiffness properties. The mathematic model of Type 1 IC HPS has been derived by Wu based on the rules of force balance, volume conservation, and the polytrophic process of gas [19], and will be summarized following, which will be utilized to establish the AMEsim model.

Ignoring the inertia force of the movement parts and mass of structure, the output forces of struts can be evaluated through:

$$F_i = P_{1i}A_{1i} - P_{3i}A_{3i} + F_{fi}sign(\dot{x}_i) \quad (i = L, R) \quad (1)$$

where P_{1i} and P_{3i} represent the pressure of MC and AC, respectively; A_{1i} and A_{3i} are the area of MC and AC respectively; F_{fi} is the seal friction of struts; $\dot{x}_i$ is the velocity of main piston, and downward direction is defined as positive direction.

Based on the volume conservation and ignoring the fluid compressibility, the fluid flow can be expressed as:

$$Q_{1L} = -Q_{12L} - Q_{1L3R} \quad (2a)$$
$$Q_{1R} = -Q_{12R} - Q_{1R3L} \quad (2b)$$
$$Q_{3L} = -Q_{1R3L} \quad (2c)$$
$$Q_{3R} = -Q_{1L3R} \quad (2d)$$

where Q_{1i} and Q_{3i} $(i = L,R)$ are the fluid flow rates in MC and AC, respectively; Q_{12i} $(i = L,R)$ are the fluid flow rate from MC to RC; $Q_{1i3j}(i = L$ or $R; j = R$ or $L)$ represents the fluid rate through the hydraulic pipes between MC of strut i and AC of strut j.

Assuming the pressure variations between MC and RC can be expressed as:

$$Q_{12L} = C_d n_{12L} a_{12L} \sqrt{\frac{2|P_{1L} - P_{2L}|}{\rho}} sign(P_{1L} - P_{2L}) \quad (3a)$$

$$Q_{12R} = C_d n_{12R} a_{12R} \sqrt{\frac{2|P_{1R} - P_{2R}|}{\rho}} sign(P_{1R} - P_{2R}) \quad (3b)$$

where C_d is the flow coefficient; n_{12i} and $a_{12i}(i = L, R)$ are the number and area of orifices between MC and RC of struts; $P_{2i}(i = L, R)$ are the pressure of RC of struts.

Assuming laminar fluid flow through the interconnected pipes, the fluid flow across the interconnected pipes can be expressed as:

$$Q_{1L3R} = \frac{\pi D^4}{128\mu L}(P_{1L} - P_{3R}) \quad \text{and}$$

$$Q_{1R3L} = \frac{\pi D^4}{128\mu L}(P_{1R} - P_{3L}) \quad (4)$$

where D and L are the diameter and length of interconnected pipes; μ is the dynamic viscosity of fluid.

The flow rate in MC and AC of each strut can be obtained through the velocities of the main pistons, $\dot{x}_l$ and $\dot{x}_r$, as:

$$Q_{1L} = -\dot{x}_L \cdot A_{1L}; \quad Q_{1R} = -\dot{x}_R \cdot A_{1R};$$
$$Q_{3L} = \dot{x}_L \cdot A_{3L}; \quad Q_{3R} = \dot{x}_R \cdot A_{3R} \quad (5)$$

Therefore, the velocity of floating piston can be obtained from (2) and (5) as:

$$\dot{x}_{fL} = (A_{1L}\dot{x}_L - A_{3R}\dot{x}_R)/A_{4L} \quad \text{and}$$
$$\dot{x}_{fR} = (A_{1R}\dot{x}_R - A_{3L}\dot{x}_L)/A_{4L} \quad (6)$$

where $\dot{x}_{fi}$ $(i = L, R)$ is the velocity of the floating piston related to the top of main piston.

Following the polytrophic process of ideal gas, the pressure of GC (P_{4i}) can be expressed as:

$$P_{4i}V_{4i}^n = P_{0i}V_{0i}^n \quad (i = L, R) \quad (7)$$

where n is polytropic index; V_{4i} is the volume of GC; V_{0i} and P_{0i} are the initial gas volume and pressure of GC, respectively.

The above established equations of motion did not consider the fluid compressibility, which is widely accepted by researchers [19], [25], [26]. As the main purpose of this study is to investigate and verify the basic dynamic properties of these types of IC HPS by experiment, the compressibility of the oil has been ignored as well.

B. MODELING OF TYPE 2 IC HPS

The single HPS design, which composes the proposed Type 2 IC HPS, was introduced by Wu [19]. Comparing with that for Type 1 IC HPS, the flow can move between MC and AC through orifices in strut. Except the above issue, Type 1 and Type 2 IC HPS are similar.

Based on the above, one can easily find that the flow conservation equation should consider the added flow path between MC and AC in the Type 2 IC HPS design as:

$$Q_{1L} = -Q_{12L} - Q_{13L} - Q_{1L3R} \quad (8a)$$
$$Q_{1R} = -Q_{12R} - Q_{13R} - Q_{1R3L} \quad (8b)$$
$$Q_{3L} = Q_{1R3L} + Q_{13L} \quad (8c)$$
$$Q_{3R} = Q_{1L3R} + Q_{13R} \quad (8d)$$

where Q_{12i} $(i = L, R)$ are the fluid flow rate from MC to AC.

The pressure variations across the orifices between MC and AC can be expressed as:

$$Q_{13L} = C_d n_{13L} a_{13L} \sqrt{\frac{2|P_{1L} - P_{3L}|}{\rho}} sign(P_{1L} - P_{3L}) \quad (9a)$$

$$Q_{13R} = C_d n_{13R} a_{13R} \sqrt{\frac{2|P_{1R} - P_{3R}|}{\rho}} sign(P_{1R} - P_{3R}) \quad (9b)$$

where n_{13i} and a_{13i} are the number and area of orifices between MC and AC of struts, respectively.

From (5) and (8), the following fluid flow relationship can be obtained:

$$Q_{12L} + Q_{12R} = \dot{x}_L \cdot A_{2L} + \dot{x}_R \cdot A_{2R} \quad (10)$$

where A_{2i} $(i = L, R)$ is the area of piston rod, as shown in Fig. 1. Apart from the above, the other equations related to Type 2 IC HPS are similar to those for Type 1.

III. EXPERIMENTAL AND SIMULATION

In this section, the experimental setup will be presented in detailed, which includes the selected testing signals. At the same time, the simulation model based on the AMEsim software will also be established. The dynamic properties of these two types of IC HPS will be evaluated and analyzed based on the experiments and simulation results.

A. EXPERIMENTAL SETUP

In order to investigate the dynamic properties of these two types of IC HPS, the prototypes have been designed and manufactured, and then tested on MTS structural dynamic test system, as shown in the Fig. 2. The design parameters and characteristics of these two types of IC HPS have been summarized in Table 1.
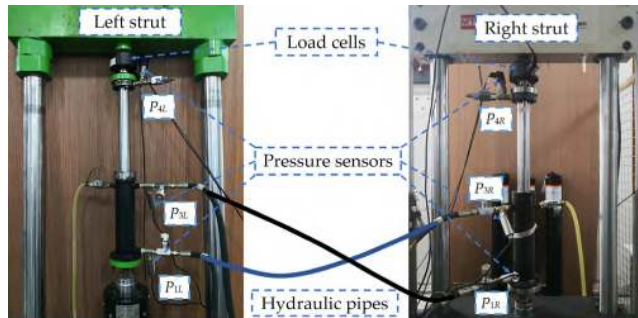

FIGURE 2. Experimental platform.

TABLE 1. Design parameters and experimental setting of IC HPS.

Definition	Description	Value
n_{12l}, n_{12r}	Number of orifices between the main and rod oil chamber	10
n_{13l}, n_{13r}	Number of orifices between the main and annular oil chamber (only in Type 2)	22
a_{12l}, a_{12r} (mm^2)	Area of orifice between main and rod oil chamber	3.10
a_{13l}, a_{13r} (mm^2)	Area of orifice between main and annular oil chamber (AC)	1.70
A_{1l}, A_{1r} (mm^2)	Area of the main piston	3117
A_{2l}, A_{2r} (mm^2)	Area of the strut rod	1590
A_{3l}, A_{3r} (mm^2)	Area of the annular chamber (AC)	1527
A_{4l}, A_{4r} (mm^2)	Area of the floating piston	962
D (mm)	Diameter of interconnected hydraulic pipes	6
L (mm)	Length of interconnected hydraulic pipes	2500
P_0 (MPa)	Initial charge pressure at the full extension condition	0.44
h_0 (mm)	Initial testing position of the two struts	73.8

It should be noted that the prototypes are identical, except that the orifices between MC and AC on the Type 2 IC HPS, as shown in Fig. 1. Two adjustable flow valves (max 6 mm diameter) were installed at the end of each pipe. The struts were installed on the MTS 849 test system and one established test platform based on the MTS 248 hydraulic actuator, respectively. The rod of struts was fixed to an inertial beam through a 10 kN force sensor. Six pressure sensors (0-10 MPa) were installed to measure oil/gas pressure in MC, AC and GC chambers of each strut, as illustrated in Fig. 2. The displacement of each strut was measured by a Linear
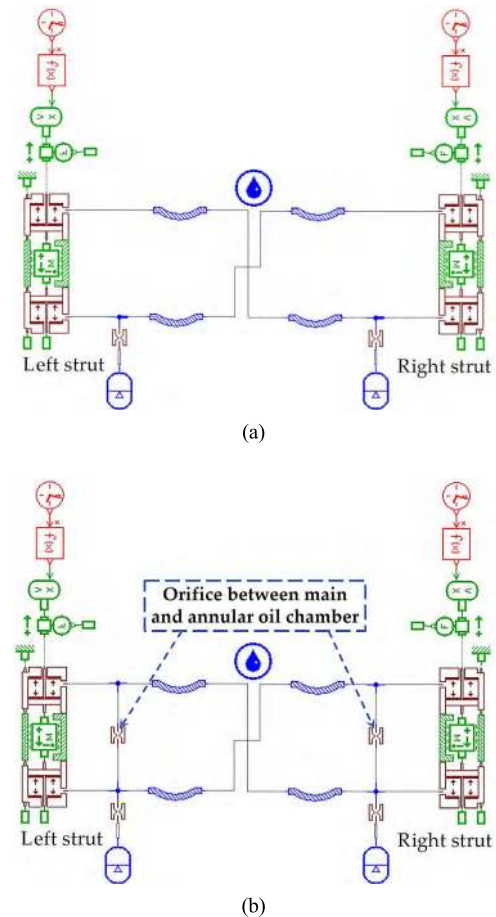

FIGURE 3. The established simulation model based on AMEsim software: (a)Type 1 IC HPS; (b)Type 2 IC HPS.

Variable Differential Transformer (LVDT) integrated within actuator. The gas temperature was measured by a thermocouple installed inside the GC. The initial charging gas pressure was 0.44 MPa, when the struts were fully extended under room temperature (30°). The middle position of struts is set to be 73.8mm (compressed from the full-extended position), and the recorded total force is 1850 N at room temperature (30°).

B. AMEsim MODELING OF 2 TYPES OF IC HPS

Based on the equations of motion derived on section II, and structural schematic shown on the Figs. 1 and 2, and Table 1, the AMEsim models of these two types of IC HPS have been established, as presented in Fig. 3. Here, it should be noted that the friction properties utilized in the established AMEsim model is the combination of the stiction friction force (350N), the Coulomb friction force (350N), the stick displacement threshold (0.1mm), and time constant (0.0001s), which is the available command combined in the AMEsim software and the parameters are selected based on the experimental data.

C. EXPERIMENT

Two series experiments based on the harmonic signal were designed to analyze the pressure/force – displacement/velocity properties of these two types of IC HPS.

Definition	Description	Value
n	Ploytropic index	1.4
C_d	Flow coefficient	0.7
$\mu(\text{Ns/m}^2)$	dynamic viscosity of fluid	0.6

The first series experiment is the in-phase test, and the peak velocity is 200 mm/s (1Hz-31.83mm, 1.5Hz-21.22mm, 2Hz-15.92mm). The second one is the out-of-phase test (180° phase deviation), and the signal can be expressed as:

$$x_L = B\sin(2\pi ft - \pi/2); \quad x_R = B\sin(2\pi ft + \pi/2) \quad (11)$$

where B and f are the amplitude and frequency of the harmonic excitation. In this situation, the left strut (L) is on the position of maximum extension ($-B$), and the right strut (R) is on the position of maximum compression (B) at the beginning of the test.

It has been found from the experiment that the output force of Type 1 IC HPS will be extremely high in the out-of-phase working condition, which will be analyzed in the following sections. Therefore, the experiment for out-of-phase test is limited to 7.96mm with 1 Hz and 2Hz, and then the detailed dynamic analysis will be conducted based on the experiment and AMEsim model together.

IV. RESULTS

The main purpose of this section is to present and analyze the basic properties of these two types of IC HPS, and verify the validity of the established simulation model based on AMEsim software. Here, it should be noted that the data presented in the following sections is based on the left strut (L) of the IC HPS shown in Fig. 1, as both sides are identical.

A. DYNAMIC PROPETIES UNDER IN-PHASE WORKING CONDITION

Fig. 4 presents the experimental data for the force - displacement/velocity properties of two types of IC HPS under the first series test signal, as presented in subsection III-C.

It can be found from Fig. 4 that the maximum output force and stiffness of Type 1 IC HPS is higher than those of Type 2 IC HPS. This is mainly due to the facts that adding one additional path, one additional path between MC and AC in the Type 2 design, in an enclosed hydraulic system will make the system become soft. The output force for Type 2 IC HPS is always positive, and the maximum and minimum output force will be found in the neighborhoods of the points of full compression and extension, which are directly related to the maximum and minimum pressure of GC (P_4), respectively.

However, one can also find three special phenomena for Type 1 IC HPS in Fig. 4: (a) the maximum output force is obtained before the point of full compression (zero velocity/maximum displacement); (b) the F-$\dot{x}$ curve shows the distortion during the compression procedure; (c) the output force will go to the negative value in the extension procedure,
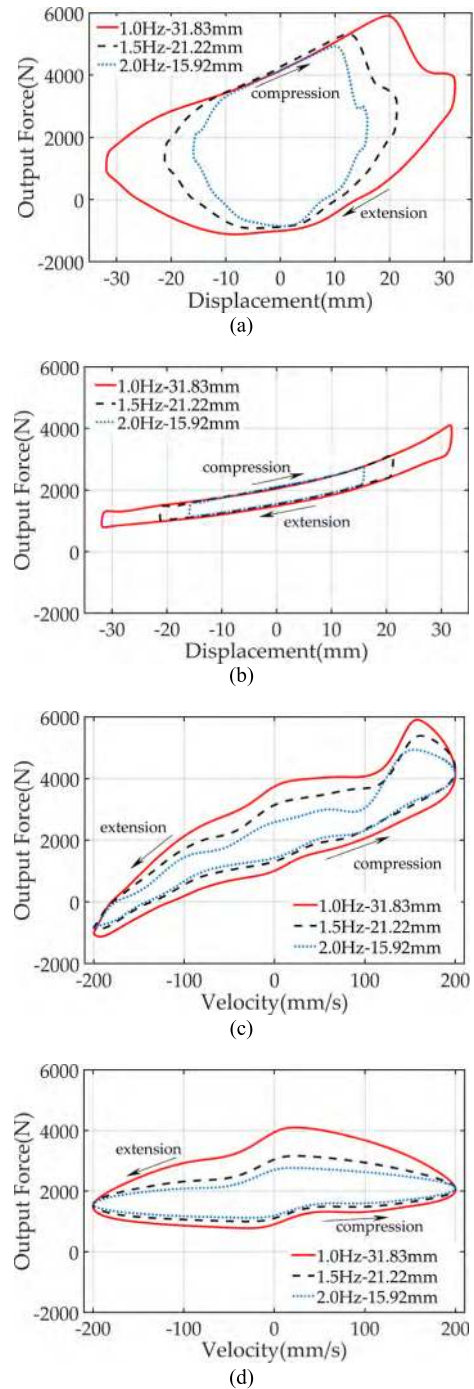

FIGURE 4. Experimental data of two types of IC HPS based on the first series test signal: (a) $F_L - x$ for Type 1; (b) $F_L - x$ for Type 2; (c) $F_L - \dot{x}$ for Type 1; (d) $F_L - \dot{x}$ for Type 2.

and the maximum negative value happens around the point of minimum velocity. Based on the researcher's investigation, the above phenomenon did not be reported in the available literatures, and then they will be analyzed in detailed in this study.

As presented in section II, the system output force is directly related to the pressure between MC and AC, and the
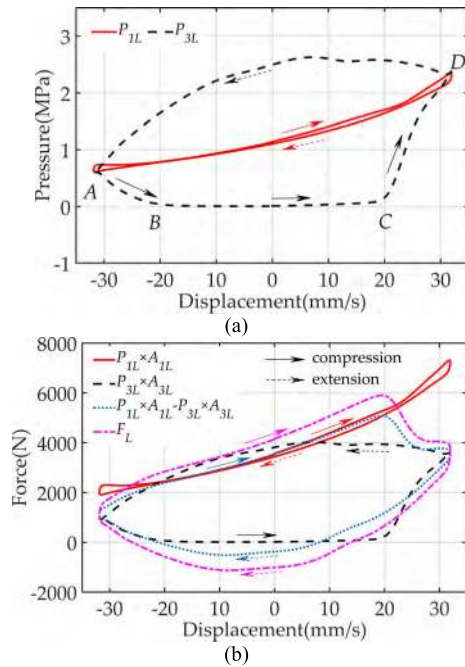
FIGURE 5. Experimental data for (a) main chamber pressure(P_{1L})/annular chamber pressure(P_{3L})-displacement; (b) $P_{1L} \times A_{1L}$, $P_{3L} \times A_{3L}$, $P_{1L} \times A_{1L} - P_{3L} \times A_{3L}$, and output force F_L - Displacement (Type 1 IC HPS).

friction. Let us examine the pressure of P_{1L} and P_{3L}, as illustrated in Fig. 5(a), and the value of $P_{1L} \times A_{1L}$, $P_{3L} \times A_{3L}$, $P_{1L} \times A_{1L} - P_{3L} \times A_{3L}$, and output force F_L for Type 1 IC HPS, as illustrated in Fig. 5(b).

One can find from Fig. 5(a) that along the compression procedure: (a) from Point A to B, as the delay(block) of fluid flow in the interconnected pipes, the flow from MC of right strut to the AC of left strut cannot effectively fill the AC chamber ($Q_{3L} - Q_{1R3L} \geq 0$). And then the pressure of AC (P_{3L}) will decrease slowly toward the vacuum section. Therefore, the output force and $P_{1L} \times A_{1L} - P_{3L} \times A_{3L}$, as presented in (1), will increase, as shown in Fig. 4(a); (b) from point B, cavitation happens in the AC, and it goes to the vacuum section (at around 170mm/s)[27]. Therefore, $P_{1L} \times A_{1L} - P_{3L} \times A_{3L}$, the output force (ignoring the friction), from Point B to C will almost follow the curve of $P_{1L} \times A_{1L}$, as shown in Fig. 5(b); (c) after point C, with the decrease of the excitation velocity, the fluid will fill the AC quickly, as AC is on the almost vacuum condition, and then P_{3L} will increase fast, as shown in Fig. 5(a). Therefore, $P_{1L} \times A_{1L} - P_{3L} \times A_{3L}$ and the output force will drop sharply, as shown in Fig. 4(a) and Fig. 5(b), respectively. After fully charging, the fluid flow returns to the normal working condition, and then the pressure of AC increases slowly toward point D, as shown in Fig. 5. Here, it should be noted that from Point B to C, one can observe that the P_{3L} increase slowly after the point close to the maximum velocity, this is mainly due to the leaking of the seal between MC and AC, which will be discussed based on the AMEsim model in subsection IV-C.

From Point D to A is the extension procedure, the output force goes to negative value at the neighbor of middle position, as the value of $P_{1L} \times A_{1L}$ smaller than $P_{3L} \times A_{3L}$, as shown in Fig. 5(b). Based on the above description, the mentioned three phenomena for Type 1 IC HPS are mainly related to the delay(block) of the fluid flow in interconnected pipes, which will be discussed in detailed in the next section.

B. DYNAMIC PROPETIES UNDER OUT-OF-PHASE (180° PHASE DEVIATION) WORKING CONDITION

Fig. 6 presents the experimental data for the force - displacement/velocity properties of Type 1 and 2 IC HPS under the second series test signal, as presented in subsection III-C.

Again, it can be found from Fig. 6 that: (a) that the maximum output force and stiffness of Type 1 IC HPS is higher than those of Type 2 IC HPS; (b) the stiffness and damping of the Type 2 IC HPS is almost zero, and the curve of force-velocity shows that its properties is only related to the friction. This is mainly due to the fact that at this excitation with low peak velocity (100mm/s), in the Type 2 IC HPS the sum of fluid flows in/between MC and AC of two struts ($\sum_{i=L,R} Q_{1i} + Q_{3i}$) is almost zero, and then almost not pushing the floating piston, which can be found from the pressure curve of the gas chamber, as illustrated in Fig. 7. One can easily realize that this kind of dynamic properties of the Type 2 IC HPS design is unacceptable for practical applications. It will be shown in the next section that through adjusting the size of orifices and interconnected pipes, the dynamic properties of the Type 2 IC HPS can be modified significantly.

For the Type 1 IC HPS design, the output force will change from around -2000 to 4000 N, and do not have significant change under the second series test signal (7.96 mm amplitude) with 1 and 2 Hz excitation frequencies. This is mainly due to the fact that in the initial condition, $P_{4R} \gg P_{4L}$ and this large pressure difference will make the filling procedure from MC to AC between both sides of struts more efficient, and then avoid the block condition in the interconnected pipes, as mentioned in the in-phase test shown in subsection IV-A. No block in the interconnected pipes will also avoid the cavitation and then the output force distortion, as presented in the last subsection. Therefore, the maximum and minimum output force are mainly related to the compression of the gas chamber. It should be noted that with the increase of the excitation peak velocity, the block condition may happen, which will be discussed in the next section.

It can also be found from Fig. 6 that for the Type 1 IC HPS design the output force (a) can go to around 4000 N under low excitation amplitude (7.96mm); (b) will go to the negative value at extension procedure. The first phenomenon is mainly due to the facts that under this design the fluid utilized to push the gas chamber (L or R) is the summation of those from MC (L or R) and AC (R or L), as fluid flow rate equation presented in (6). Therefore, considering the safety reason, only limited experiment has been conducted in this design.

For Type 1 IC HPS, the negative output force can be explained by the equation of system output force,
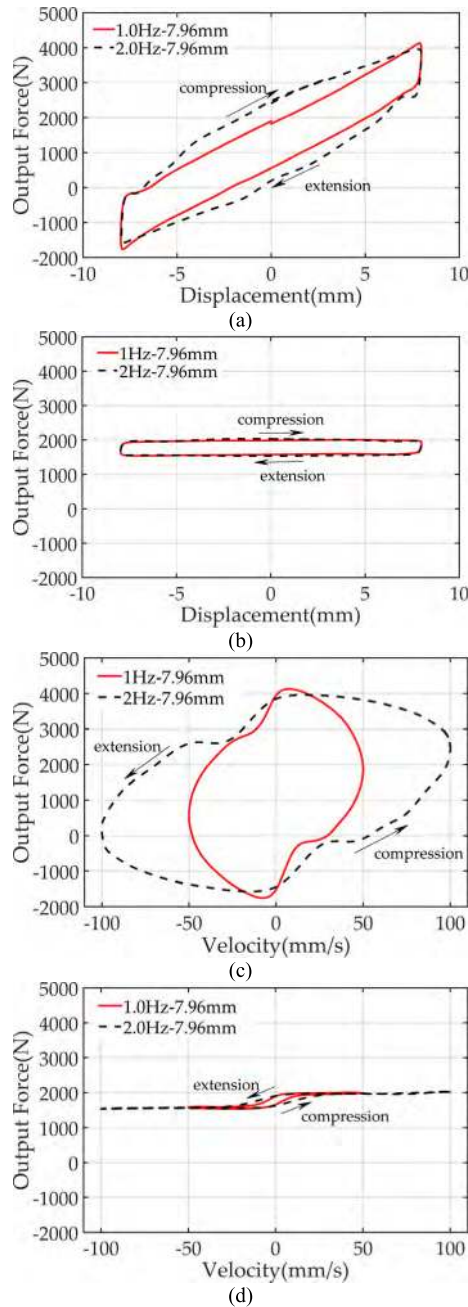
FIGURE 6. Experimental data of two types of IC HPS based on the second series test signal: (a) $F_L - x$ for Type 1; (b) $F_L - x$ for Type 2; (c) $F_L - \dot{x}$ for Type 1; (d) $F_L - \dot{x}$ for Type 2.

FIGURE 7. Experimental data of gas chamber pressure(P_{4L}) - displacement for(a) Type 1 IC HPS;(b) Type 2 IC HPS.

as illustrated in (1). Focusing on the left strut, the output force can be expressed as $P_{1L} \times A_{1L} - P_{3L} \times A_{3L}$, and the pressure of AC (P_{3L}) is related to the pressure of MC on the right strut (P_{1R}). Therefore, for out-of-phase test, the condition of $P_{3L} \times A_{3L}$ higher than $P_{1L} \times A_{1L}$ can be expected, especially from the beginning of the extension procedure.

C. AMESIM MODEL

The AMEsim model has been established to evaluate the dynamic properties of these two types of IC HPS.
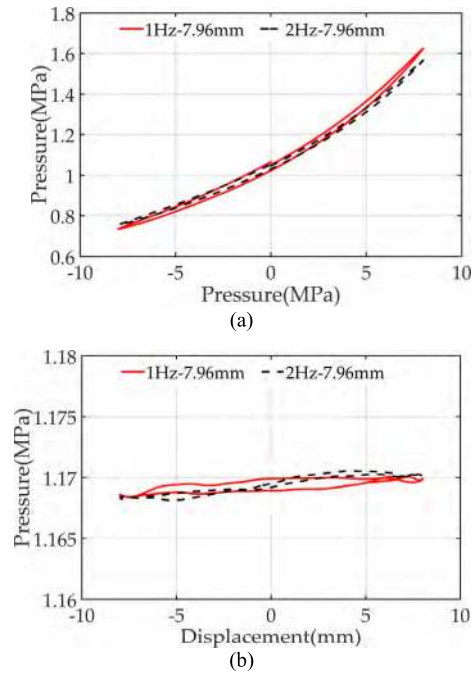
Fig. 8 illustrates the result of output force-displacement curve obtained from experiment and the simulation based on the AMEsim model for the two series test signal, as presented in subsection III-C. It can be found from Fig. 8 that the established AMEsim model can catch the dynamic properties of the prototypes with good agreement, although these two types of IC HPS show complicated dynamic properties, as mentioned in the above two subsections.

The main difference between experiment and model can be observed: (1) in the area of around the maximum output force at the compression procedure of Type 1 IC HPS for the first series test, (2) in the maximum displacement area of Type 2 IC HPS for the second series test.

The first difference is mainly due to the leaking between MC and AC, as shown in Fig. 9, which compares the pressure of AC (P_{3L}) obtained from experiment and AMEsim model. Because of leaking, in the compress procedure, under high working pressure the experiment shows that P_{3L} will increase slowly after the vacuum section, as mentioned in subsection IV-A and shown in Fig. 5 (a). AMEsim model do not consider this leaking, and then P_{3L} will keep vacuum condition until the excitation velocity drops to some value, which will allow the MC of the other strut to charge AC efficiently. Definitely, adding one path in the enclose hydraulic system will soften the system, which has been illustrated in Fig. 8 that the maximum output force of experiment is smaller than AMEsim model. In the extension procedure, the main piston pushes the fluid flowing out of AC, and considering the delay of the interconnected pipes, the fluid will leak from AC to MC, especially the negative output
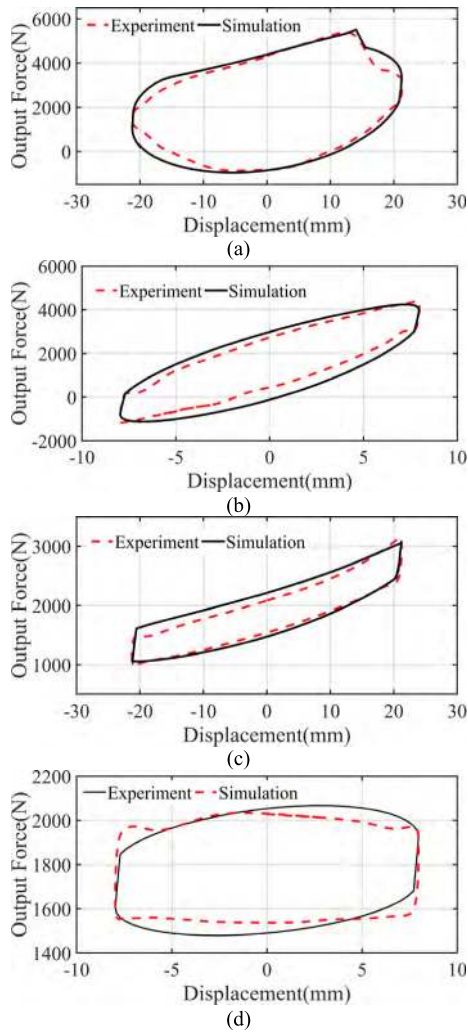
FIGURE 8. Comparisons of the experimental and simulated curve of output force (F_L)-displacement (x): (a) Type 1 (1.5Hz-21.22mm, in-phase); (b) Type 1 (2Hz-7.96mm, out-of-phase); (c) Type 2 (1.5Hz-21.22mm, in-phase); (d) Type 2 (2Hz-7.96mm, out-of-phase).

FIGURE 9. Comparison of the AC pressure (P_{3L}) between experimental and simulated data.

FIGURE 10. The simulated output force - displacement for Type 2 IC HPS under 2Hz-7.96mm and 2Hz-11.93mm excitations, out-of-phase.

force section, as shown in Fig. 4. Therefore, in the whole extension procedure, the value of P_{3L} of AMEsim model is always higher than that of experiment. Here, it should be noted that as the main purpose of this research paper is to compare and reveal the fundamental dynamic properties of Type 1 and 2 HPS shown in Fig. 1, the detailed investigation of the leakage will be the topic of the future research work.

The second difference is mainly due to the friction of seal. In the established AMEsim model, the packed friction model has been selected. For Type 2 IC HPS, because of its small output force, the effectiveness of the friction will become obvious.

V. DISCUSSION
Based on the result and analysis of the dynamic properties of these two types of IC HPS presented in section IV, this section will be focused on the effect of the strut parameters to the dynamic properties, special emphasis will be put on
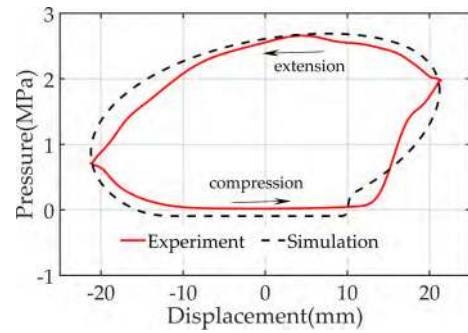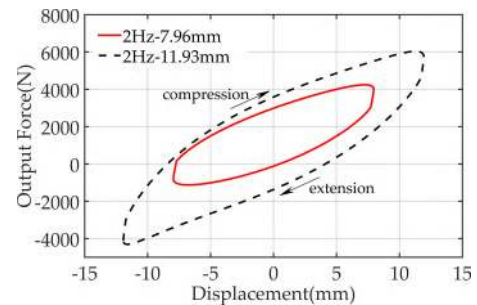
those phenomena presented in section IV. As mentioned in section III, only small amplitude (7.96mm) harmonic test signal has been conducted for the second series test. This is mainly due to the extreme output force for Type 1 IC HPS, which has been explained in subsection IV-B. Fig. 10 illustrates the comparison of the output force for Type 1 IC HPS under harmonic excitation with excitation frequency, 2 Hz, and amplitude 7.96 and 11.93mm based on the AMEsim model. It can be found from Fig. 10 that under the same frequency, small change of amplitude will result in a huge difference on output force of Type1 IC HPS. Therefore, for the safety reason, in the experiment for the second series test, only small amplitude has been selected, and the dynamic properties discussion, to be presented in this section, will be based on the AMEsim model under harmonic test signal with 11.93mm amplitude.

A. EFFECT OF INTERCONNECTED PIPES
Based on the result shown in section IV, one can find that lots of phenomenon is directly related to the fluid flow delay/block in the interconnected pipes, and then this section will mainly analyze the effect of interconnected pipes through changing the diameter and the length.

1) THE LENGTH OF INTERCONNECTED PIPES
Fig. 11 illustrates the simulated result of dynamic properties of these two types IC HPS for different length (2 m, 2.5 m, 3 m) of interconnected pipes based on AMEsim model.
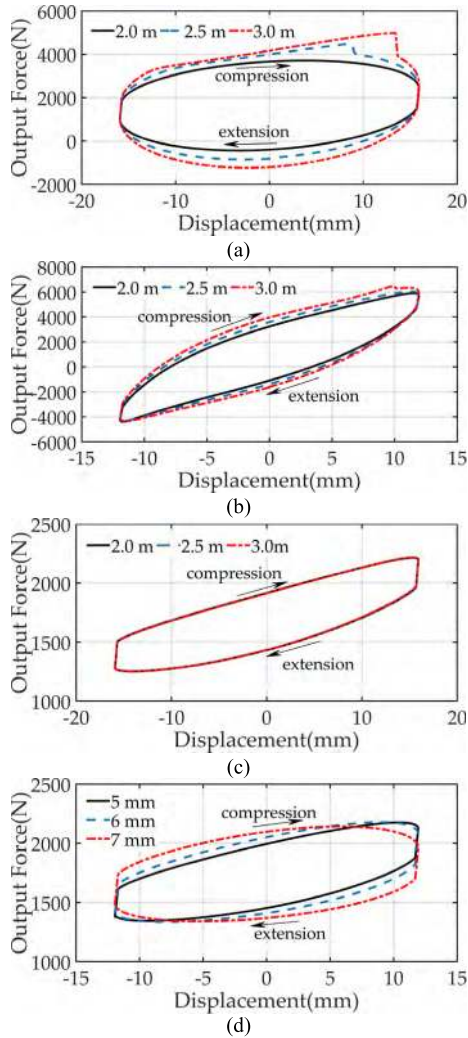
FIGURE 11. The simulated output force- displacement data with different length of connection pipes (2.0 m, 2.5 m, 3.0 m): (a)Type 1 (2Hz-15.92mm, in-phase); (b) Type 1 (2Hz-11.93mm, out-of-phase); (c) Type 2 (2Hz-15.92, in-phase); (d) Type 2 (2Hz-11.93mm, out-of-phase).

FIGURE 12. The simulated pressure of AC (P_{3L}) – displacement of Type 1 IC HPS with different length of connection pipes (2.0 m, 2.5 m, 3.0 m): (a) 2Hz-15.92mm, in-phase; (b) 2Hz-11.93mm, out-of-phase.

The harmonic excitation with 15.92 mm amplitude and 2 Hz frequency is applied to the in-phase test, and 11.93 mm amplitude and 2 Hz frequency for out-of-phase test.

Fig. 11(a) illustrates the in-phase test for Type 1 IC HPS. It can be found from Fig. 11(a) that: (a) with the decrease of the length of interconnected pipes, the output force distortion phenomenon in the compression procedure, which is mainly due to the cavitation in the AC, and is directly related to the block of the fluid flow in the interconnected pipes, as discussed in the subsection IV-A, will become small and disappear. To demonstrate this point, Fig. 12(a) illustrates the pressure of AC (P_{3L}), from which one can easily find that the P_{3L} will leave the vacuum section with the decrease of length of the interconnected pipes; (b) the maximum output force will decrease with the decrease of length of interconnected pipes. This is due to fact that shorter interconnected pipes will make smaller delay or avoid block, and let P_3 of one side strut
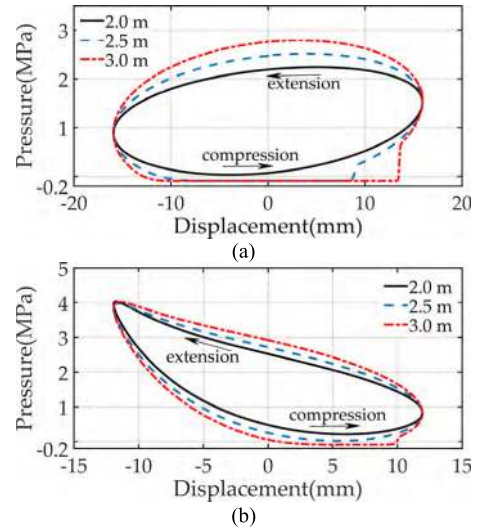
can catch the P_1 of the other side, and then avoid cavitation. Therefore, the output force shown in (1) will become small.

Fig. 11(b) illustrates dynamic properties for the out-of-phase test for Type 1 IC HPS, from which it can be found that the output force will increase with the increase of the length of interconnected pipes, but not have significant change. It is because that (a) with the increase of the length of interconnected pipes, the fluid flow delay will increase, and then P_3 will increase and decrease in the compression and extension procedure, respectively, as illustrated in Fig. 12(b); (b) huge pressure difference between P_{3L} and P_{1R} at the initial condition will faster the fluid flow in the interconnected pipe, and then slow down the cavitation condition in the AC. Therefore, the maximum output force is almost directly related to the displacement and happen at the point of the maximum displacement. In fact, one can observe from Fig. 11 (b) that small output force distortion happens for the 3 m length of the interconnected pipes, and then the maximum output force is located before the point of maximum displacement as discussed for the in-phase test, and illustrated in Fig. 12(b), in which the P_{3L} goes to the vacuum section for 3mm length connection pipes.

Fig. 11(c) presents the dynamic properties for the in-phase test for Type 2 IC HPS. It can be found that (a) as one extra fluid path added in Type 2 IC HPS, the output force is smaller than those for Type 1 IC HPS;(b) the extra fluid path will make the fluid flow in the system smooth, and then the output force shows almost not change for different length of the interconnected pipes.

Fig. 11 (d) illustrates the dynamic properties for the out-of-phase test for Type 2 IC HPS, from which it can be found that with the increase of length of interconnected pipes, the curve of output force vs displacement will (a) become narrow, which can be observed from the difference of the output force
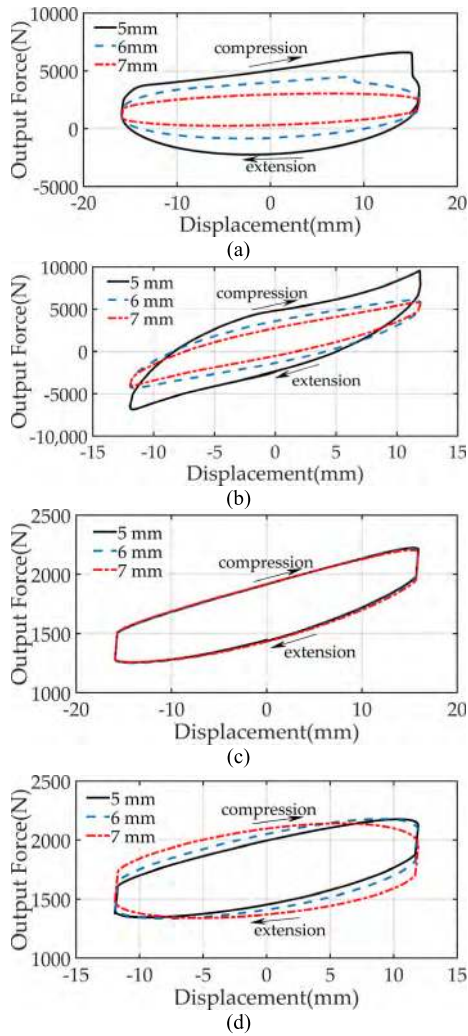
FIGURE 13. The simulated output force-displacement data with different diameters of connection pipes (5mm, 6mm, 7mm): (a)Type 1 (2Hz-15.92mm, in-phase); (b) Type 1 (2Hz-11.93mm, out-of-phase); (c) Type 2 (2Hz-15.92mm, in-phase); (d) Type 2 (2Hz-11.93mm, out-of-phase).

FIGURE 14. The simulated output force data with different number (2, 5, 10, 20) of 2mm orifice for Type 2 IC HPS: (a) $F_L - x$ (2Hz-15.92mm, in-phase); (b) $F_L - x$ (2Hz-15.92mm, in-phase); (c) $F_L - \dot{x}$ (2Hz-15.92mm, out-of-phase); (d) $F_L - \dot{x}$ (2Hz-15.92mm, out-of-phase).

at the maximum velocity points between the compression and the extension procedures. Besides, it is mainly due to the increase of the damping with the increase of length of interconnected pipes; (b) turn counter-clockwise, which is also related to the fact that the increase of block with the increase of the length of interconnected pipes will increase the system stiffness.

2) THE DIAMETER OF INTERCONNECTED PIPES

Fig. 13 presents the simulated result of dynamic properties of these two types IC HPS for different diameters (5 mm, 6 mm, 7 mm) of interconnected pipes based on AMEsim model. The harmonic excitation with 15.92 mm amplitude and 2 Hz frequency is applied to the in-phase test, and 11.93 mm amplitude and 2 Hz frequency for out-of-phase test.

Comparing Fig. 13 with those shown in Fig. 11, one can find that the trend of the dynamic properties of these two
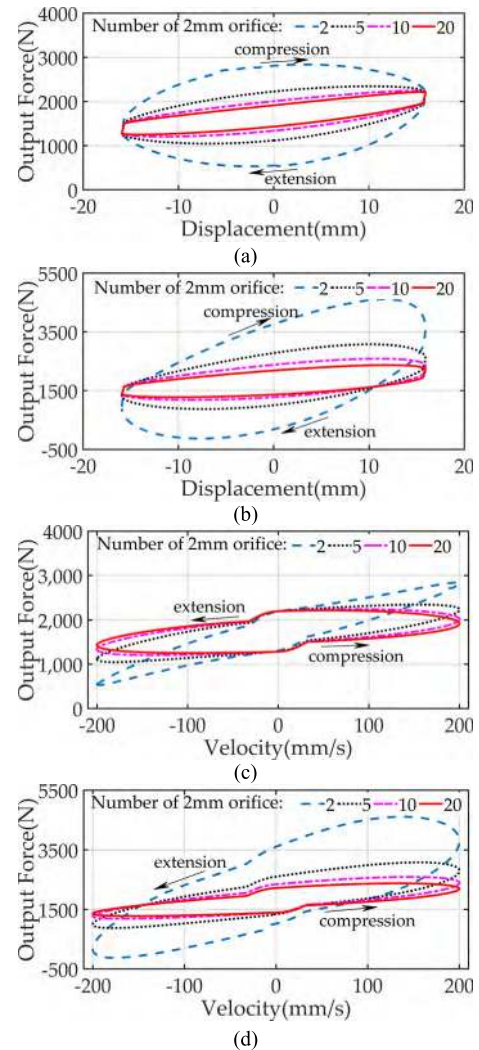
types of IC HPS with the changing of the diameters of the interconnected pipes are agreed with those for the length of the interconnected pipes, but with opposite direction, and more significant. This is due to fact that the delay of fluid flow in the interconnected pipes can be evaluated by (4), from which one can realize that the effective of the diameter is power 4 and positive direction, comparing with those for the length, which is the linear and opposite.

B. THE ORIFICES BETWEEN MAIN AND ANNULAR CHAMBERS OF TYPE 2 IC HPS

As mentioned in section IV-A and section IV-B, that the dynamic properties of Type 2 IC HPS show small stiffness (almost zero stiffness and damping in the out-of-phase condition). This is not suitable for practical applications. In subsection V-A, it has been illustrated that through changing the length and diameter of the interconnected pipes the stiffness
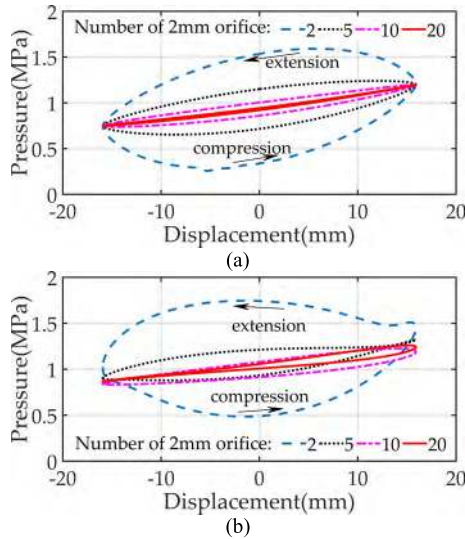
FIGURE 15. The simulated pressure of annular chamber with different number (2, 5, 10, 20) of 2mm orifice for Type 2 IC HPS: (a) $P_{3L} - x$ (2Hz-15.92mm, in-phase); (b) $P_{3L} - x$ (2Hz-15.92mm, out-of-phase).

of Type 2 IC HPS can be modified. This subsection will focus on the effectiveness of orifice between MC and AC to the stiffness and damping properties. Fig. 14 illustrates the dynamic properties under different number of orifices.

From Fig. 14, one can find that the stiffness and damping properties of Type 2 IC HPS can be effectively improved with the modification of the orifice between MC and AC. Besides, comparing with those for Type 1 IC HPS, it can be realized that Type 2 IC HPS can avoid the cavitation condition (distortion phenomenon in the compression procedure) in AC, as shown in Fig. 15 for the pressure of AC (P_{3L}).

VI. CONCLUSION

In this study, the dynamic properties of two types of IC HPS have been investigated based on set-up experiment on the designed prototypes and the established simulation model based on the AMEsim software. The result shows that the established simulation model can catch the experiment with good agreement, and then the dynamic analysis and discussion were conducted on the basis of the experiment and simulation model together.

The result shows output force distortion condition and negative output force situation for Type 1 IC HPS. It has been illustrated that the above phenomenon is directly related to the delay/block of the fluid flow in the interconnected pipes, and can be modified through selecting shorter or larger diameter interconnected pipes. However, for the out-of-phase working condition, the negative output force condition will always be meet, except decreasing the area of the Annular Chamber.

For Type 2 IC HPS, it shows similar dynamic properties comparing with those for single strut system for in-phase working condition, and low stiffness properties for out-of-phase test. It has been verified that the stiffness can be adjusted through selecting longer and smaller diameter inter-

connected pipes, but the most efficient way is to narrow the orifices between Main Chamber and the Annular chamber. The result suggests that Type 2 IC HPS not only has ability to provide suitable stiffness and damping properties, but also is able to avoid the cavitation phenomenon in annular chamber through properly designed orifice between main and annular oil chamber.

The presented work provides the fundamental investigation on two types of interconnected hydro-pneumatic struts. The results suggest that the Type 2 IC HPS has great potential application in the area of vehicle suspension system. Therefore, future investigation will be placed on: (a) the leakage properties based on the experimental data; (b) the modification of the dynamic properties of Type 2 IC HPS through variable orifice between main chamber and annular or diameter in the connection pipes base on the experimental data, and their sensitive analysis [28]; (c) investigation of the full vehicle model with consideration of the roll/pitch mode based on the established IC HPS model.

REFERENCES

[1] Z. Wang, Y. Qin, C. Hu, M. Dong, and F. Li, "Fuzzy observer-based prescribed performance control of vehicle roll behavior via controllable damper," *IEEE Access*, vol. 7, pp. 19471–19487, 2019.

[2] H. Zhang, J. Liu, E. Wang, S. Rakheja, and C. Y. Su, "Nonlinear dynamic analysis of a skyhook-based semi-active suspension system with magneto-rheological damper," *IEEE Trans. Veh. Technol.*, vol. 67, no. 11, pp. 10446–10456, Nov. 2018.

[3] F. Zhao, S. S. Ge, F. Tu, Y. Qin, and M. Dong, "Adaptive neural network control for active suspension system with actuator saturation," *IET Control Theory Appl.*, vol. 10, no. 14, pp. 1696–1705, Sep. 2016.

[4] L. Liu, Y.-J. Liu, and S. Tong, "Neural networks-based adaptive finite-time fault-tolerant control for a class of strict-feedback switched nonlinear systems," *IEEE Trans. Cybern.*, vol. 49, no. 7, pp. 2536–2545, Jul. 2019.

[5] S. Wen, M. Z. Q. Chen, Z. Zeng, X. Yu, and T. Huang, "Fuzzy control for uncertain vehicle active suspension systems via dynamic sliding-mode approach," *IEEE Trans. Syst., Man, Cybern., Syst.*, vol. 47, no. 1, pp. 24–32, Jan. 2017.

[6] L. Liu, Y. J. Liu, and S. Tong, "Fuzzy based multi-error constraint control for switched nonlinear systems and its applications," *IEEE Trans. Fuzzy Syst.*, to be published. doi: 10.1109/TFUZZ.2018.2882173.

[7] M. C. Smith and G. W. Walker, "Interconnected vehicle suspension," *Inst. Mech. Eng., D, J. Automobile Eng.*, vol. 219, no. 3, pp. 295–307, Mar. 2005.

[8] F. Saglam and Y. S. Unilusory, "Modelling and simulation of a three-axle vehicle with interconnected hydro- pneumatic suspension system," in *Proc. 36th FISITA World Automot. Congr.*, Bursan, Korea, Sep. 2016, Art. no. F2016-VDCA-035

[9] D. Cao, S. Rakheja, and C. Y. Su, "Dynamic analyses of heavy vehicle with pitch-interconnected suspensions," *Int. J. Heavy Veh. Syst.*, vol. 15, no. 4, pp. 272–308, Jan. 2008.

[10] W. A. Smith and N. Zhang, "Recent developments in passive interconnected vehicle suspension," *Frontiers Mech. Eng.*, vol. 5, no. 1, pp. 1–18, Mar. 2010.

[11] N. Rosam and J. Darling, "Development and simulation of a novel roll control system for the interconnected hydragas suspension," *Vehicle Syst. Dyn.*, vol. 27, no. 1, pp. 1–18, Jul. 1997.

[12] Y. Hou, H. Song, M. Ma, J. Xiao, and N. Zhao, "The stiffness characteristics study on an interconnected anti-rolling suspension system," in *Proc. Int. Conf. Mech. Eng. Contr. Syst.*, Washington, DC, USA, Jan. 2015, pp. 79–82.

[13] N. Zhang, W. A. Smith, and J. Jeyakumaran, "Hydraulically interconnected vehicle suspension: Background and modelling," *Vehicle Syst. Dyn.*, vol. 48, no. 1, pp. 17–40, Jan. 2010.

[14] W. A. Smith, N. Zhang, and W. Hu, "Hydraulically interconnected vehicle suspension: Handling performance," *Vehicle Syst. Dyn.*, vol. 49, nos. 1–2, pp. 87–106, Feb. 2011.

[15] F. Ding, X. Han, N. Zhang, and Z. Luo, "Characteristic analysis of pitch-resistant hydraulically interconnected suspensions for two-axle vehicles," *J. Vib. Control*, vol. 21, no. 16, pp. 3167–3188, Dec. 2014.

[16] F. Ding, N. Zhang, J. Liu, and X. Han, "Dynamics analysis and design methodology of roll-resistant hydraulically interconnected suspensions for tri-axle straight trucks," *J. Franklin Inst.*, vol. 353, no. 17, pp. 4620–4651, Nov. 2016.

[17] Q. Yao, X. Zhang, K. Guo, Y. Yang, and J. Feng, "Study on a novel dual-mode interconnected suspension," *Int. J. Vehicle Des.*, vol. 68, no. 4, pp. 81–103, 2015.

[18] Q. Lam, L. Wang, and N. Zhang, "Experimental implementation of a fuzzy controller for an active hydraulically interconnected suspension on a sport utility vehicle," in *Proc. Intell. Veh. Symp.*, Jul. 2013, pp. 283–390.

[19] L. Wu, "Analysis of hydro-pneumatic interconnected suspension struts in the roll plane vehicle model," M.S. thesis, Dept. Mech. Indus. Eng., Concordia Univ., Quebec, Canada, 2003.

[20] Z. Zhang, S. Cao, and C. Ruan, "Statistical linearization analysis of a hydropneumatic suspension system with nonlinearity," *IEEE Access*, vol. 6, pp. 73760–73773, 2018.

[21] N. Jiao, J. Guo, and S. Liu, "Hydro-pneumatic suspension system hybrid reliability modeling considering the temperature influence," *IEEE Access*, vol. 5, pp. 19144–19153, 2017.

[22] D. Cao, S. Rakheja, and C. Y. Su, "Dynamic analyses of roll plane interconnected hydro-pneumatic suspension systems," *Int. J. Vehicle Des.*, vol. 47, no. 4, pp. 51–80, Jan. 2008.

[23] D. Cao, S. Rakheja, and C. Y. Su, "Roll- and pitch-plane-coupled hydro-pneumatic suspension. Part 2: Dynamic response analyses," *Vehicle Syst. Dyn.*, vol. 48, no. 4, pp. 507–528, Aug. 2010.

[24] D. Cao, "Theoretical analyses of roll- and pitch-coupled hydro-pneumatic strut suspensions," Ph.D. dissertation, Dept. Mech. Indus. Eng., Concordia Univ., Quebec, Canada, 2008.

[25] N. J. Theron and P. S. Els, "Modelling of a semi-active hydropneumatic spring–damper unit," *In. J. Vehicle Design*, vol. 45, no. 4, pp. 501–521, 2007.

[26] F. Ding, X. Han, Z. Luo, and N. Zhang, "Modelling and characteristic analysis of tri-axle trucks with hydraulically interconnected suspensions," *Vehicle Syst. Dyn.*, vol. 50, no. 12, pp. 1877–1904, Jun. 2012.

[27] W. Tian, S. Jiao, B. Yang, and W. Wang, "Simulation and Distortion Analysis of Hydro-pneumatic Suspensions," *Noise Vehicle Control*, vol. 36, no. 5, pp. 70–74, 2016.

[28] Y. Qin, Z. Wang, C. Xiang, M. Dong, C. Hu, and R. Wang, "A novel global sensitivity analysis on the observation accuracy of the coupled vehicle model," *Vehicle Syst. Dyn.*, to be published. doi: 10.1109/TTHZ.2016.2544142.

DI GONG received the B.E. degree (Hons.) in mechanical engineering and automation from Shanghai University, in 2016. He is currently pursuing the Ph.D. degree with the College of Mechanical Engineering and Automation, Huaqiao University, Xiamen, Fujian, China. His research interests include mechatronics, vibration control, and smart materials.

FENG ZHAO received the B.E. degree in power mechanical engineering from the University of Shanghai for Science and Technology, China, in 1986, and the M.S. degree in mechanical engineering from Concordia University, Montreal, QC, Canada, in 1999. He is currently a Senior Research Fellow with the College of Mechanical Engineering and Automation, Huaqiao University, Xiamen, Fujian, China. His research interests include mechatronics, robotic control, and artificial intelligence.

XIANGYU LUO received the Ph.D. degree in computer science from Sun Yat-sen University, in 2006. He is currently an Associate Professor with the College of Computer Science and Technology, Huaqiao University. His main research interests include model checking, multi-agent systems, temporal logics, and epistemic logics. He has been involved in the national project of model checking for multi-agent systems.

DEZHAO LIN received the B.E. degree (Hons.) in mechanical engineering from Huaqiao University, Xiamen, Fujian, China, in 2017, where he is currently pursuing the master's degree with the College of Mechanical Engineering and Automation. His research interests include vibration control and vehicle suspension.

RUIHONG LI received the B.E. degree (Hons.) in mechanical engineering from Huaqiao University, Xiamen, Fujian, China, in 2018, where he is currently pursuing the master's degree with the College of Mechanical Engineering and Automation. His research interests include vibration control and vehicle dampers.

FAN YANG received the B.E. degree (Hons.) in aerospace engineering from the Civil Aviation University of China, in 1996, and the M.S. and Ph.D. degrees in mechanical engineering from Concordia University, Montreal, QC, Canada, in 2004 and 2008, respectively. He was a Postdoctoral Research Fellow and a Research Associate with Concordia University, from 2009 to 2011, and then, he was appointed as an Associate Professor with the South China University of Technology. He is currently with the College of Mechanical Engineering and Automation, Huaqiao University, Xiamen, Fujian, China, where he has been a Professor. His research interests include mechatronics, vibration control, and the application of smart material actuators and dampers.

ZHIHONG LIN received the M.S. degree in naval architecture and marine engineering from Jimei University, in 2016. He is currently pursuing the Ph.D. degree with the College of Mechanical Engineering and Automation, Huaqiao University, Xiamen, Fujian, China. His research interests include mechatronics, vibration control, and the application of smart material dampers.

• • •